ELSEVIER

Thermochimica Acta 314 (1998) 281–289

thermochimica acta

The use of metastable phase diagrams in primary crystallization kinetics study

M.T. Clavaguera-Mora*

Grup de Física de Materials I, Departament de Física, Universitat Autònoma de Barcelona, 08193-Bellaterra, Spain

Received 6 October 1997; accepted 12 January 1998

Abstract

Metastable multiphase materials are currently obtained by controlled crystallization of amorphous samples. This paper deals with the use of metastable equilibrium phase diagrams and related thermodynamic quantities to the kinetic analysis of primary crystallization of an undercooled liquid solution as obtained by calorimetric means. The analysis is performed as a function of the processing conditions, assuming thermodynamic and kinetic competition between several crystalline phases for nucleation and growth. The hierarchy of crystalline phases formation on both heating an initial amorphous alloy or on cooling the liquid solution follows a sequence mostly consequent with the different temperature dependence of the several quantities driving crystal formation. © 1998 Elsevier Science B.V.

Keywords: Crystallization; Soft impingement; Differential scanning calorimetry; Nucleation and growth of primary crystals

1. Introduction

Metastable multiphase materials are currently obtained by controlled heat treatment that induces a partial crystallization in disordered samples, either amorphous or molten alloys. In the present paper we will consider phase transformations in which the new phase can not completely replace the parent disordered phase because of a difference in composition. It will thus give rise to a mixture of primary crystals and remaining disordered phase in metastable equilibrium. The decisive factor for the progress of primary crystallization is the supply of nuclei, since the composition of the emerging and growing nuclei differs from that of the disordered phase [1,2]. Therefore, the thermodynamic mechanism limiting the spread of the transformation is the Gibbs free energy difference between crystals and remaining disordered phase [3,4], whereas the kinetic mechanism limiting the transformation is diffusion. The use of the Gibbs free energy diagrams of the possible metastable competing phases provides a basis for classifying the possible composition ranges in which crystallization can proceed. Since there is a crystallization enthalpy, calorimetric methods, in particular differential scanning calorimetry (DSC), are currently being used for the study of the kinetics of the process.

There exists a wide bibliography related to phase transformations focused on the thermodynamic, calorimetric and kinetic aspects (see Refs. [4–11]). However, the theory of primary crystallization kinetics at present has not yet been developed to a satisfactory level, despite recent efforts and progress made in elucidating the kinetics of first-order phase transformation in solids. In the present paper, the main

*Corresponding author. Fax: 0034 3581 1564/63; e-mail: mtmora@vega.uab.es

PII S0040-6031(98)00264-0

advances will be reviewed as well as current assumptions with regards to the thermodynamic and calorimetric analysis of kinetic data. The plan of presentation is the following. In Section 2 the concept of primary crystallization will be introduced phenomenologically. In Section 3 the thermodynamics of multicomponent alloys and metastable phase equilibria involving the liquid phase will be analysed. In Section 4 the kinetics of the process, as visualised by calorimetric means, will be discussed. Finally, discussion of the interplay among kinetic, calorimetric and thermodynamic data will be discussed and some conclusion drawn in Section 5.

2. Primary crystallization

In primary crystallization (or in precipitation of a second phase) the composition of the emerging and growing nuclei differs from that of the disordered (or crystalline) parent phase. We will consider that crystallization, as well as solidification, deals with the transformation undercooled liquid⇒crystal. The composition of the remaining disordered matrix evolves during the transformation. The treatment is performed under the hypothesis that at the end of the transformation there is a metastable equilibrium between the primary crystals and the remaining disordered matrix. This implies that the nucleation frequency of the primary phase in the disordered matrix becomes negligible at the end of the transformation. That is, the nucleation frequency depends on the degree of advancement of the process. Immediately after nucleation, the stable nucleus is embedded into a still supersaturated matrix. It may be argued that for small particles the interface reaction is likely to be the rate controlling step, since the diffusion distances are very short. Once the particles have grown to a certain size, the surrounding matrix composition approaches saturation and the associated reduction in the driving force makes diffusion likely to be the rate controlling step [1,2,6,9].

At any time, t, the transformation proceeds up to a fraction, $x{\cdot}f_1$, of the total volume, V, where f_1 is the total volume fraction available for primary crystallization and x is the degree of advancement of the process. According to the well known Johnson–Mehl–Avrami–Kolmogorov theory [12–14], when no stable nuclei were present in the parent phase the time evolution of the crystallized fraction, x, is given by

$$x(T,t) = 1 - \exp\left[-\int_0^t I(\tau)v(t,\tau)\ \mathrm{d}t\right] \qquad (1)$$

where $I(\tau)$ is the nucleation frequency at time τ and $v(t,\tau)$ is the extended volume at time t of nuclei formed at time τ, both quantities being implicitly dependent on the processing conditions, namely both of them depend on the degree of advancement and on the time dependence of the temperature $T=T(t)$ during the process. The integration of Eq. (1) allows to obtain the forms $x=x(T,t)$ or $x=x(T,\beta)$ if the particular heat treatment applied to the sample is isothermal or at a constant heating (cooling) rate, β, respectively [15,16].

The nucleation frequency, I, is computed assuming the classical theory for homogeneous nucleation [17,18], that is:

$$I = I_o \exp[-16\pi\sigma^3/3RT(\Delta G)^2] \qquad (2)$$

with

$$I_o = N_v kT/3\pi a_o^3 \eta \qquad (3)$$

where N_v is the mean fraction of atoms in the liquid, a_o is the mean atomic diameter,

$$\eta = A\ \exp[B/(T - T_\eta)] \qquad (4)$$

η is the viscosity, T the absolute temperature, T_η is the Vogel-Fulcher temperature, σ is the crystal–liquid interfacial energy, and ΔG the Gibbs free energy difference between the liquid and the crystal. Among all these parameters, the thermodynamic important ones are ΔG and σ. The evaluation of ΔG for primary crystallization will be discussed in Section 3 whereas σ is difficult to evaluate and, normally, is only estimated. Some interfacial energies of pure metals have been calculated by Turnbull [18,19] and Perepezko [20,21].

The presence of heterogeneous nucleation results in a reduction of the energy barrier for nucleation by a factor $f(\theta)$, whose dependence on the wetting angle θ is [22]

$$f(\theta) = \frac{(2 + \cos\theta)(1 - \cos\theta)^2}{4} \qquad (5)$$

The transient time needed to attain the quasi-steady

distribution of embryos, t_o, may be of short duration compared with the period of observation. Otherwise, the nucleation rate, including the transient effect, may be written as [6]

$$I_t \approx I \exp(-t_o/t) \tag{6}$$

With regards to the evaluation of the extended volume, $v(t,\tau)$, at time t of nuclei formed at time τ, the growth rate is currently assumed either interface or diffusion controlled. Growth rate, u, under interface controlled growth is expressed by

$$u = u_o[1 - \exp\{-(\Delta G/RT)\}] \tag{7}$$

with

$$u_o = fkT/3\pi a_o^2\eta \tag{8}$$

where f is the fraction of crystal sites on the nucleus surface where atoms are preferentially added.

Diffusion controlled spherical growth under steady state conditions is often taken to produce a growth velocity of the form [23]

$$\frac{dr}{dt} \approx \frac{c^o - c^*}{c^{xt} - c^*}\frac{D}{r} \tag{9}$$

with c^* and c^o the matrix concentration at and far from the interface, c^{xt} that of the crystalline precipitate, D the volume diffusion coefficient and r the crystalline grain radius.

Primary crystallization may be visualised as initiated by the formation of stable nuclei via 'heterophase' thermal composition fluctuations (see Fig. 1(a)). A thermodynamic analysis of concentration fluctuations and homogeneous nucleation of crystal in undercooled binary alloys has been presented by Desre [24]. He showed that the undercooling needed to form nuclei of critical composition and size is rather low compared to that needed to get partitionless solidification.

In the early stages the stable nucleus is surrounded by a still supersaturated matrix. When the liquid at the interface reaches equilibrium composition diffusion becomes the limiting growth mechanism (Fig. 1(c)). At intermediate stages the system consists of a polydispersed mixture of precipitates of various sizes; the matrix is enriched from atoms insoluble in these grains and the associated reduction in the concentration gradient slows grain growth. At the final stages the metastable equilibrium between the primary precipitates and the remaining matrix is ideally attained (Fig. 1(f)). That is, there is an initial transient, for each individual grain growth, in which the local equilibrium in between the emerging crystal and the

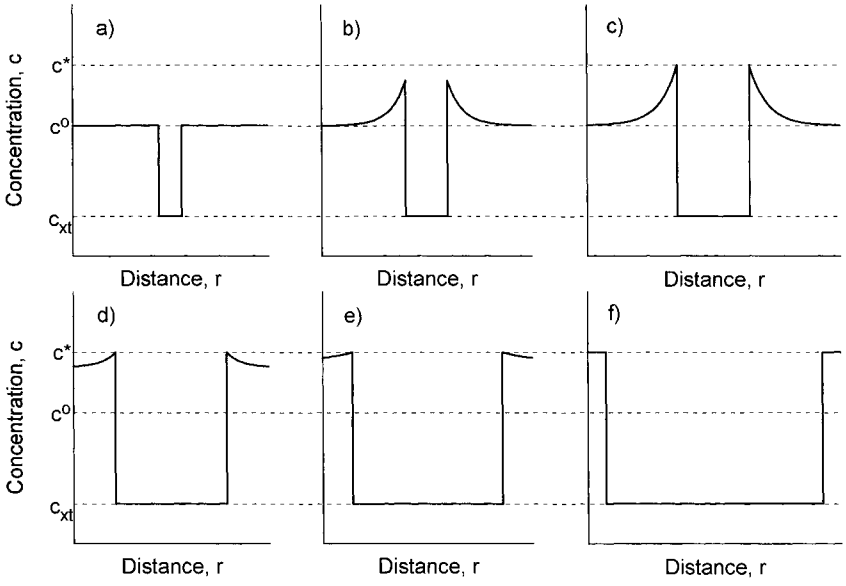

Fig. 1. Schematic view of the extended growth of an individual grain.

liquid ahead of the crystal–liquid interface is established; afterwards, diffusion becomes the controlling mechanism. Two cases are currently distinguished: (i) low degrees of supersaturation: $c^{xt}-c^{o}>>c^{o}-c^{*}$; (ii) high degrees of supersaturation: $c^{xt}-c^{o}\ll c^{o}-c^{*}$. According to the continuous change in composition of the remaining liquid during primary crystallization, low degrees of supersaturation are always reached in the course of the transformation. Soft impingement, then, may be formally included by replacing c^{o} in Eq. (9) by $c(t)$, that is, assuming that the primary grains are growing not in an infinite matrix, but in a liquid whose concentration tends to a mean value, $c(t)$, in regions remote from the interface. Another effect to be included in primary crystallization is the change of the nucleation frequency of primary crystals along the transformation.

3. Thermodynamics of multicomponent systems

The main thermodynamic quantities needed to solve the kinetic Eqs. (2),(7) and (9) are ΔG, σ, c^{xt} and c^{*} as a function of temperature and composition of the parent liquid, c^{o}, for all possible competing phases, that is, far away from the range of stability of most of the phases. This is the reason why their evaluation requires to predict the possible metastable equilibria with methods like the CALPHAD approach or others.

For a binary system, in Fig. 2 there is a schematic view of how ΔG may evolve during the transformation, assumed to proceed under isothermal conditions. We will comment the figure in connection with Fig. 1. At low degrees of advancement of the transformation, as shown in Fig. 1(a), the stable nucleus emerges from a matrix whose composition in very close to c^{o}. That is, the value of ΔG to be introduced in Eq. (2) is represented by the value ΔG^{a} shown in Fig. 2(a). At intermediate values of the degree of advancement, the stable nuclei emerge from a matrix whose composition, $c(t)$, ranges in between c^{o} and c^{*}; then the value of ΔG needed to evaluate the homogeneous nucleation frequency becomes ΔG^{b}, shown in Fig. 2(b). The consideration of crystal growth is not simple. As schematised in Fig. 1, there is a growth-transient from nucleus formation until the achievement of local equilibrium with the surrounding liquid at the grain interface (from situations depicted in Fig. 1(a) to (c)). During this growth-transient, the interplay between interface and diffusion limited growth acts in a way to increase the importance of the last mechanism until it becomes preponderant. Strictly speaking, the value of ΔG to be used in Eq. (7) depends on the matrix composition at the interface. It changes with the degree of advancement of the transformation and evolves also with increasing grain size. That is, at the initial stages of growth, it ranges from ΔG^{a} (shown in Fig. 2(a)) at low degrees of advancement of the transformation, to ΔG^{b} (Fig. 2(b)) as crystallization proceeds. But, at large degree of advancement of the transformation, it is given by ΔG^{b} after nucleus formation and, consequently, the transient time to reach

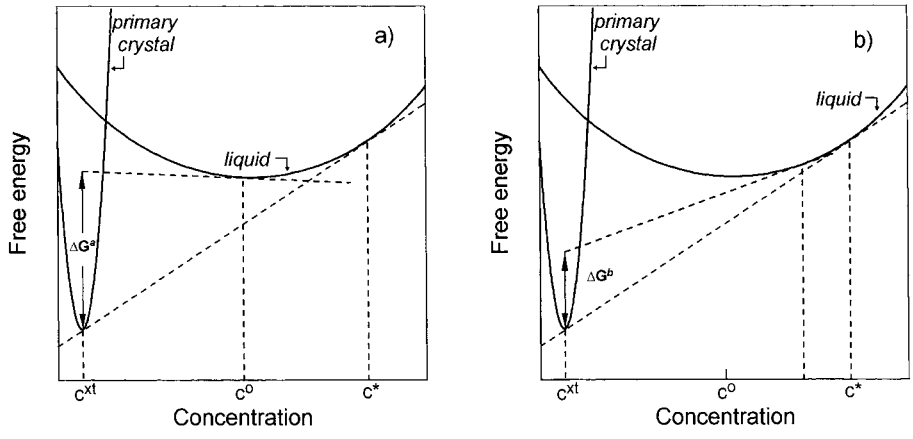

Fig. 2. Gibbs free energy schematic plot of the liquid and primary phase at a given temperature T.

the situation depicted in Fig. 1(c) is shortened. The second stage of individual grain growth, in the extended view i.e. neglecting spatial impingement between grains, may be approximately represented, instead of Eq. (9), by a diffusion controlled growth of the form

$$\frac{dr}{dt} \approx \frac{c(t) - c^*}{c^{xt} - c^*} \frac{D[c(t)]}{r} \tag{10}$$

provided the precipitates form under low degrees of supersaturation. At high degrees of supersaturation, the growth-transient stage may last for enough time to reduce the importance of diffusion controlled growth in the overall crystallization process.

All the previous discussion becomes more complex for multicomponent systems. The evaluation ΔG is straightforward, and is formally given by the following expression [3,4]

$$\Delta G(\boldsymbol{x}^{xt}, \boldsymbol{x}^{liq}, T) = \sum_{i=1}^{c} \boldsymbol{x}_i^{xt} \cdot [\mu_i^{xt}(\boldsymbol{x}^{xt}, T) - \mu_i^{liq}(\boldsymbol{x}^{liq}, T)] \tag{11}$$

where $\boldsymbol{x}^{\phi}$ denotes the set of atomic fractions x_i^{ϕ} (i=1,2,...c) of each component i in phase ϕ and μ_i^{ϕ} its chemical potential at temperature T. For the calculation of the nucleation rate, the liquid composition refers to the mean value, $c(t)$, in regions remote from the interface. For the evaluation of the interplay between interface and diffusion controlled growth, the liquid composition refers to the local value of the surrounding matrix at the interface with the extended crystalline grain.

The use of metastable phase equilibrium predictive diagrams is very helpful for the evaluation of ΔG by Eq. (11). The main difficulty arises in the evaluation of the changes of supersaturation for each component and, thus, of the driving forces for nucleation and growth processes. Most effort has been devoted to the development of the treatment of the diffusional problem. In particular, Zener [25], Wert and Zener [26] and Ham [27] describe the time evolution of precipitates with uniform size introducing the overlapping concentration profile between precipitates. But, the interpretation of experimental kinetic data through the thermodynamic characterization of the respective alloy systems and underlying free energy curves remains quite restrictive. It has been, for instance, successively attempted to analyse glass-forming ability [28–30].

4. Calorimetric analysis

Calorimetric crystallization kinetic studies have been performed most frequently under continuous heating conditions, probably because only differential thermal analysis techniques were available in the past. As very sensitive DSC equipments become available, they are widely used as a tool to study kinetics of transformation. Today, coupled isothermal and continuous heating calorimetric measurements allow the determination of the explicit form of the rate of reaction versus temperature/time as a function of both the heating rate/temperature and the fraction of already transformed material. These measurements allow the determination of the explicit form of the evolution of transformed material versus time as a function of both the temperature and the fraction of already transformed material [11]. Measurement under continuous heating is rather straightforward, but isothermal measurements are time consuming and can be performed only in a limited temperature range because of the thermally activated nature of the process. Nevertheless, there are limits to the accuracy on the determination of the rate of reaction, one of the most important being the uncertainty on the base line position. Other sources of error come from both the difficulty to avoid base line instability during the experiment and the incertitude on the exact position of the onset and end of the transformation peak (or any other thermal event) in the DSC curve. Both effects are specially important under isothermal conditions but also in continuous heating regime [11,31].

The specificity of primary crystallization introduces other sources of difficulty to directly extract the rate of reaction from the measured calorimetric signal. As already mentioned, at any stage of the crystallization process, the respective values of the concentration in the crystal and at the interface are established from the free energy diagrams. During the transformation, the volume fraction occupied by the primary crystals is $x \cdot f_1$, where f_1 is given by the lever rule,

$$f_1 = (c^* - c^o)/(c^* - c^{xt}) \tag{12}$$

Neglecting differences of density between the various

coexisting phases, f_1 is also the mass fraction transformed at the end of the crystallization process. The calorimetric signal, namely, the heat flux evolving from the sample is

$$\dot{Q} = \Delta\dot{H} \tag{13}$$

where, in a first approximation, we have [31]

$$\Delta H = \{x \cdot f_1 \cdot H^{\mathrm{xt}}(c^{\mathrm{xt}}, T) + (1 - x \cdot f_1) \cdot H^{\mathrm{liq}}(c^{\mathrm{liq}}, T)\} - H^{\mathrm{liq}}(c^{\mathrm{o}}, T) \tag{14}$$

or, in differential form

$$\frac{\mathrm{d}\{x \cdot f_1 \cdot H^{\mathrm{xt}}(c^{\mathrm{xt}}, T)\}}{\mathrm{d}t} = \dot{x} \cdot f_1 \cdot H^{\mathrm{xt}} + x \cdot f_1 \cdot C_p^{\mathrm{xt}} \cdot \beta \tag{15}$$

$$\frac{\mathrm{d}\{(1 - x \cdot f_1) \cdot H^{\mathrm{liq}}\}}{\mathrm{d}t} = -\dot{x} \cdot f_1 \cdot H^{\mathrm{liq}} + (1 - x \cdot f_1) \cdot \left[\frac{\partial H^{\mathrm{liq}}}{\partial c} \cdot \dot{c}^{\mathrm{liq}} + C_p^{\mathrm{liq}} \cdot \beta\right] \tag{16}$$

and

$$\frac{d\{H^{\mathrm{liq}}(c^{\mathrm{o}}, T)\}}{\mathrm{d}t} = C_p^{\mathrm{liq}}(c^{\mathrm{o}}, T) \cdot \beta \tag{17}$$

In these equations H^{ϕ} and ΔC_p^{ϕ} stand for the enthalpy and heat capacity per unit mass, respectively in phase ϕ. Further, it has been assumed that the composition of the crystal, c^{xt}, remains constant all over the transformation.

Provided that: (i) $(\partial H^{\mathrm{liq}}/\partial c) \cdot \dot{c}$ is negligible, and (ii) $H^{\mathrm{liq}}[c(t)] \approx H^{\mathrm{liq}}(c^{*}) \approx H^{\mathrm{liq}}(c^{\mathrm{o}})$ and $C_p^{\mathrm{liq}}[c(t)] \approx C_p^{\mathrm{liq}}(c^{*}) \approx C_p^{\mathrm{liq}}(c^{\mathrm{o}})$ in the range $c^{\mathrm{o}} \leq c(t) \leq c^{*}$, the heat flux evolved from the sample may be divided in two terms, namely, the rate of enthalpy change of the reaction alone,

$$\dot{Q}_{\text{reaction alone}} = \dot{x} \cdot f_1 \cdot (H^{\mathrm{liq}} - H^{\mathrm{xt}}) \tag{18}$$

and the rate of sample heat capacity change from that of the undercooled liquid to that of the crystallization product,

$$\dot{Q}_{\Delta C_p} = x \cdot f_1 \cdot (C_p^{\mathrm{liq}} - C_p^{\mathrm{xt}}) \cdot \beta \tag{19}$$

Otherwise, Eqs. (18) and (19) may be considered as first order approximate expressions of the mean instantaneous heat flux generated during the reaction.

5. Primary crystallization kinetics study from thermodynamic and calorimetric data

The kinetic study of primary crystallization calorimetric data, in terms of the previously discussed approaches, has been performed for a quaternary alloy of the Al–Cu–Ni–Nd system. The alloy has nominal composition $Al_{87}Cu_3Ni_7Nd_3$ and has been prepared in ribbon form by rapid solidification. Experimental results show that nanocrystalline fcc-(Al) is formed by heating the melt spun material. The other phases which should be formed to attain equilibrium are hindered, most probably due to their negligible nucleation frequency. Experimental data also suggest the presence of pre-existing nuclei in the melt spun amorphous alloy [1,32–35]. The basic assumptions introduced in the kinetic analysis are:

A density of pre-existing nuclei observed by transmission electron microscopy.
Metastable equilibrium compositions of both the remaining untransformed phase and the precipitate given from the CALPHAD method [36–39].

In the present approach [1], the time dependence of the nucleation frequency is assumed to be of the form

$$I(\tau) = I \cdot \{1 - x(\tau)\} \tag{20}$$

with I given by Eq. (2) for the particular value of $\Delta G = \Delta G^{\mathrm{a}}$ shown in Fig. 2(a).

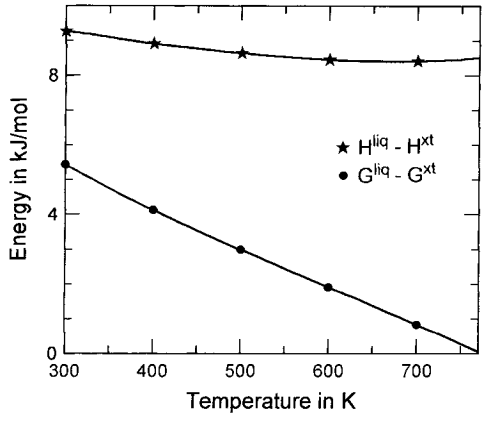

Fig. 3. Numerical values of the thermodynamic quantities used for the kinetic evaluation of the primary crystallization in alloy $Al_{87}Cu_3Ni_7Nd_3$.

This approach is grounded in the fact that when a volume $V^{xt}(t)$ of the sample becomes crystalline, a certain amount of the remaining volume is inhibited to undergo primary crystallization, its value being very close to the one established by the lever rule, namely, as $\approx V^{xt}(t) \cdot \frac{1-f_l}{f_l}$. Consequently, this is equivalent to assume for I no composition dependence provided nucleation acts in a reduced volume, V_{red}, of the total volume, V_T, given by

$$V_{red} = V_T - V^{xt} - V^{xt} \cdot \frac{1-f_l}{f_l} = V_T(1-x) \tag{21}$$

The numerical values of the Gibbs energy and enthalpy differences between the liquid and the crystal were obtained by use of THERMOCALC and are

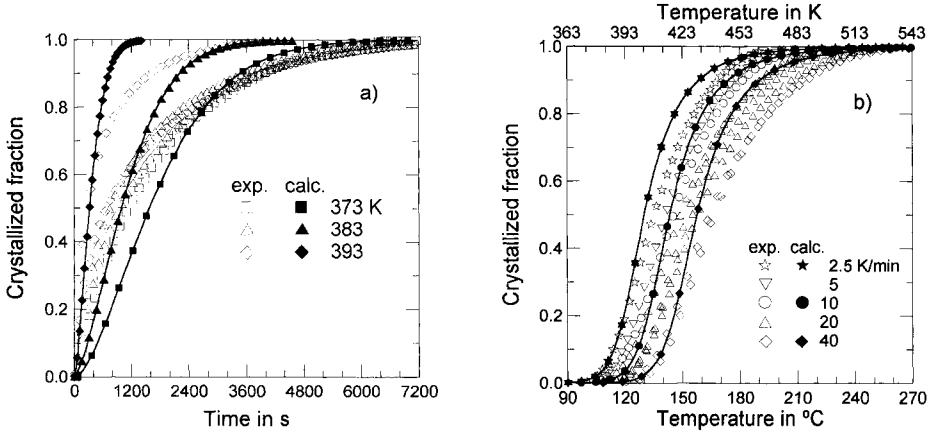

Fig. 4. Evolution of the crystallized fraction for alloy $Al_{87}Cu_3Ni_7Nd_3$: (a) under isothermal annealing; (b) under continuous heating. Modelling explained in the text, from [1].

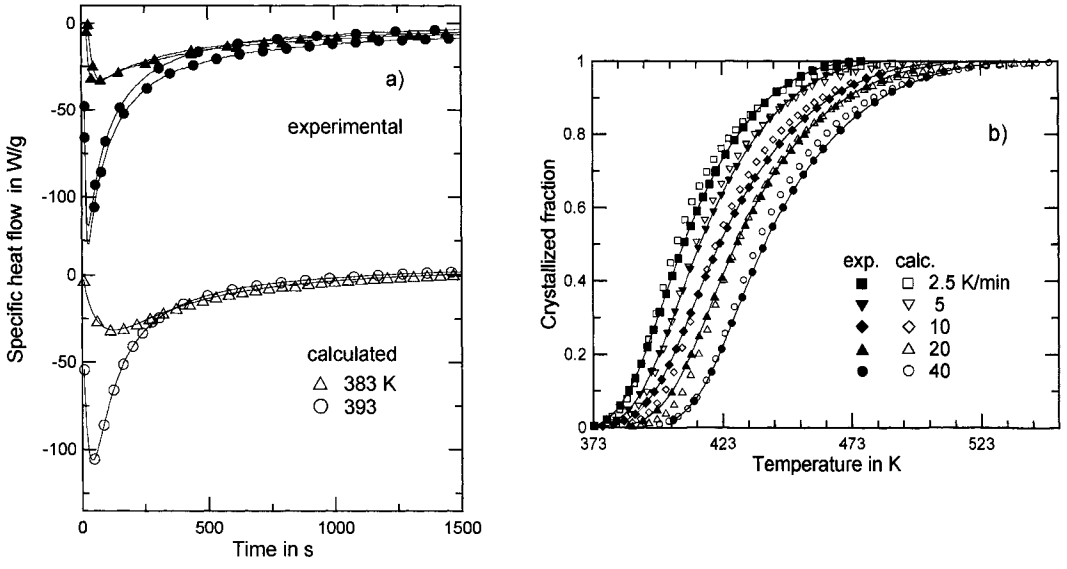

Fig. 5. Evolution of (a) the heat flow under isothermal annealing, from ref. [39]; (b) the crystallized fraction under continuous heating, for primary crystallization in alloy $Al_{87}Cu_3Ni_7Nd_3$, from ref. [40]. Evaluation of computed data explained in the text.

shown in Fig. 3. The detailed thermodynamic evaluation of the Al-rich part of the quaternary Al–Cu–Ni–Nd system is being reported elsewhere [39].

Two different approaches have been successively applied to get a semi-quantitative description of the growth mechanisms. In a first attempt [1], apart from an interface controlled growth in the early stages of the transformation, soft impingement, at any time t, was considered by use of the following simplified equation

$$\frac{\mathrm{d}r}{\mathrm{d}t} \approx \frac{c^{\mathrm{o}} - c^{*}}{c^{\mathrm{xt}} - c^{*}} \frac{D}{r} \cdot \{1 - x(t)\} \tag{22}$$

The respective experimental and calculated values of the crystallized fraction, under isothermal annealing at various temperatures and continuous heating at several values of the heating rate are presented in Fig. 4. The agreement between experimental and calculated values is qualitatively good, but there is a clear departure of the experimental data at high values of the crystallized fraction.

In a second attempt, soft impingement was taken by use of Eq. (10), including a concentration dependence for the volume diffusion coefficient, D. Also, the isothermal heat flow data $\dot{Q}$, were evaluated by use of the thermodynamic H^{liq}–H^{xt} data. The respective experimental and computed values are presented in Fig. 5. The agreement between experimental and calculated values is much improved. In particular, under isothermal regime, since the direct experimental heat flow data are compared to the computed ones, the uncertainty in the precise value at the onset/end of the transformation is avoided; for that reason the comparison is more reliable.

6. Conclusions

The metastable phase diagrams are a useful tool for the study of the hierarchy of crystalline phases formation of primary crystallization from the disordered phase as a function of the processing conditions, assuming thermodynamic and kinetic competition between several crystalline phases for nucleation and growth. Recently developed kinetic models including an approximate treatment of soft impingement may constitute an appropriate way to check the experimental data with the physical assumptions about the mechanisms which drive the process.

Acknowledgements

The authors acknowledge Professor A. Inoue (Sendai) the supply of the Al-based amorphous alloys. Financial support from projects No. 1995SGR-00514 by 'Comissió Interdepartamental de Ciència i Tecnologia' and No. MAT96-0769 from 'Comisión Interministerial de Ciencia y Tecnología' is acknowledged.

References

[1] N. Clavaguera, M.T. Clavaguera-Mora, Mat. Res. Soc. Symp. Proc. 398 (1996) 319.
[2] T. Pradell, D. Crespo, N. Clavaguera, M.T. Clavaguera-Mora, Nanostructured Materials 8 (1997) 245.
[3] E.V. Thompson, F. Spaepen, Acta Metall. 31 (1983) 2021.
[4] J.C. Baker, J.W. Cahn, Solidification, Metals Park, OH, ASM, 1971, p. 23.
[5] B.V. Yerofeev, N.I. Mitzkevitch, Reactivity of Solids, Elsevier, Amsterdam, 1961, p. 273.
[6] J.W. Christian, The Theory of Phase Transformations in Metals and Alloys, Pergamon Press, Oxford, 1965, p. 377.
[7] F. Spaepen, D. Turnbull, in: N.J. Grant, B.C. Giessen (Eds.), Proc. 2nd. Int. Conf. on Rapidly Quenched Metals, MIT Press, Cambridge, MA, 1976, p. 205.
[8] J.H. Perepezko, in: R. Mehrabian, B.H. Kear, M. Cohen (Eds.), Rapid Solidification Processing Principles and Technologies, Claitor's Publishing Division, Baton Rouge, LA., 1980, p. 56.
[9] R. Wagner, R. Kampmann, in: R.W. Cahn, P. Haasen, E.J. Kramer (Eds.), Phase Transformations in Materials, P. Haasen (volume Ed.), Materials Sci. and Techn., vol. 5, VCH, 1991, p. 213.
[10] U. Köster, U. Herold, in: H.-J. Güntherod, H. Beck (Eds.), Glassy Metals I, Springer, Berlin, 1981, p. 227.
[11] R.F. Speyer, Thermal Analysis of Materials, Marcel Dekker, Inc., New York, 1994.
[12] W.A. Johnson, K.F. Mehl, Trans. Am. Inst. Mining Met. Eng. 135 (1939) 416.
[13] M. Avrami, J. Chem. Phys. 7 (1939) 1103; 8 (1940) 212; 9 (1941) 177.
[14] A.N. Kolmogorov, Izv. Akad. Nauk. USSR, Ser. Mater. 3 (1937) 355.
[15] D.R. Uhlmann, J. Non-Cryst. Solids 7 (1972) 337.
[16] N. Clavaguera, J. Non-Cryst. Solids 162 (1993) 40.
[17] D. Turnbull, Contemp. Phys. 10 (1969) 473.
[18] D. Turnbull, J. Appl. Phys. 21 (1950) 1022.
[19] D. Turnbull, R.E. Cech, J. Appl. Phys. 21 (1950) 804.
[20] J.H. Perepezco, D.H. Rasmussen, I.E. Anderson, C.R. Lopez Jr., Solidification and Casting of Metals, The Metals Society, London, 1977, p. 169.
[21] J.H. Perepezko, in: R. Mehrabian, B.H. Kear, M. Cohen (Eds.), Rapid Solidification Processing Principles and Technologies, Claitor's Publishing Division, Baton Rouge, LA., 1980, p. 56.

[22] W. Kurz, D.J. Fisher, Fundamentals of Solidification, Switzerland, Trans. Tech. Publications, 1986.
[23] For a detailed analysis of the validity of Eq. (9) see Ref. [6].
[24] P. Desre, J. Mater. Sci. 22 (1987) 57.
[25] C. Zener, J. Appl. Phys. 20 (1949) 950.
[26] C. Wert, C. Zener, J. Appl. Phys. 21 (1950) 5.
[27] F.S. Ham, J. Phys. Chem. Solids 6 (1958) 335.
[28] F. Sommer, Z. Metallkd. 72 (1981) 219.
[29] N. Saunders, A.P. Miodownik, J. Mater. Res. 1 (1986) 38.
[30] A.P. Miodownik, Special Lecture, 14th Meeting of the Japanese Committee For Alloy Phase Diagrams, 1992.
[31] N. Clavaguera, M.T. Clavaguera-Mora, M. Fontana, J. Mater. Res. 13 (3) (1998), in press.
[32] A. Inoue, M. Yamamoto, H.M. Kimura, T. Masumoto, J. Mater. Sci. Lett. 6 (1987) 194.
[33] Y.H. Kim, A. Inoue, T. Masumoto, Mater. Trans. Jpn. Inst. Met. 31 (1990) 747.
[34] T. Masumoto, Mater. Sci. and Eng. A179/A180 (1994) 8.
[35] A. Inoue, Mater. Sci. and Eng. A179/A180 (1994) 57.
[36] L. Kaufman, H. Bernstein, Computer Calculation of Phase Diagrams, Academic Press, New York, 1970.
[37] B. Sundman, B. Jansson, B. Andersson, CALPHAD 2 (1985) 153.
[38] N. Clavaguera, Y. Du, J. Phase Equilibria 17 (1996) 107.
[39] J. Groebner, N. Clavaguera, M.T. Clavaguera-Mora, J. Phase Equilibria, submitted.
[40] N. Clavaguera, M.T. Clavaguera-Mora, D. Crespo, T. Pradell, in: J. Rivas, M.A. Lopez-Quintela (Eds.), Non-Crystalline and Nanoscale Materials, World Scientific Pub. Co. Ltd., Singapore, 1997, in press.